

Instanton constituents and fermionic zero modes in twisted \mathbb{CP}^n models

Wieland Brendel^a, Falk Bruckmann^{a,b}, Lukas Janssen^c, Andreas Wipf^c, Christian Wozar^c

^a*Institut für Theoretische Physik III, Universität Erlangen-Nürnberg, D-91058 Erlangen, Germany*

^b*Institut für Theoretische Physik, Universität Regensburg, D-93040 Regensburg, Germany*

^c*Theoretisch-Physikalisches Institut, Universität Jena, D-07743 Jena, Germany*

Abstract

We construct twisted instanton solutions of \mathbb{CP}^n models. Generically a charge- k instanton splits into $k(n+1)$ well-separated and almost static constituents carrying fractional topological charges and being ordered along the noncompact direction. The locations, sizes and charges of the constituents are related to the moduli parameters of the instantons. We sketch how solutions with fractional total charge can be obtained. We also calculate the fermionic zero modes with quasi-periodic boundary conditions in the background of twisted instantons for minimally and supersymmetrically coupled fermions. The zero modes are tracers for the constituents and show a characteristic hopping. The analytical findings are compared to results extracted from Monte-Carlo generated and cooled configurations of the corresponding lattice models. Analytical and numerical results are in full agreement and it is demonstrated that the fermionic zero modes are excellent filters for constituents hidden in fluctuating lattice configurations.

Key words: cooling, instanton, overlap operator, supersymmetry, topology, zero mode

PACS: 11.27.+d, 11.10.Wx

1. Introduction

Nonlinear sigma models in two dimensions have long been used as testing ground for strongly coupled gauge theories [1]. They are scale invariant on the classical level and asymptotically free at the quantum level. The ubiquitous \mathbb{CP}^n models possess regular instanton solutions, the topological charges of which yield lower BPS-bounds on the action, they have a chiral anomaly when coupled to fermions, generate a dynamical mass by non-perturbative effects at zero temperature and a thermal mass $\propto g^2 T$ at finite temperature. They have numerous interesting applications to condensed matter physics (for a review see [2]) and also have been used to study the sphaleron induced fermion-number violation at high temperature [3].

In the present work we consider \mathbb{CP}^n models at finite temperature, i.e., *Euclidean models* with imaginary time having period $\beta = 1/k_B T$. These models possess instanton solutions with finite action and the dimension of the moduli space in a given instanton sector depends on the topology of the Euclidean space-time. For example, on the two-torus the charge- k instantons of \mathbb{CP}^n depend on as many collective parameters as the instantons of \mathbb{CP}^{n+1} with one charge less [4]. In the present work we do not compactify space such that space-time is a cylinder.

For suitable field variables the selfduality equation for \mathbb{CP}^n instantons reduces to Cauchy-Riemann conditions such that all instantons are known explicitly for the plane, cylinder and torus. On the plane they are given by rational functions of the

complex coordinate z and on the cylinder by suitable periodic generalizations thereof, see below.

In a previous work [5] one of us introduced the twisted $O(3)$ model (which is equivalent to the \mathbb{CP}^1 model) and showed that generically the unit charged instantons in this model dissociate into two fractional charged constituents, sometimes called ‘instanton quarks’. Again there is a close analogy to the corresponding situation in Yang-Mills theories, where instantons with nontrivial holonomy along the compact direction of a four-dimensional cylinder possess magnetic monopoles as constituents [6, 7, 8, 9].

We extend the work in [5] in several directions. First we construct the $k(n+1)$ constituents of \mathbb{CP}^n instantons with charge k and twisted boundary conditions and relate their positions, sizes and fractional charges to the collective parameters of the instantons. Then we calculate and analyze the zero modes of the Dirac operator for minimally coupled fermions with quasi-periodic boundary conditions in the background of the twisted instantons. We show that the zero modes can be used as tracers for the instanton constituents: they are localized to the latter, to which constituent depends on the boundary condition. Again, this has close analogies in four-dimensional Yang-Mills theories with 1 (or 2) compact dimensions [10, 11, 12].

\mathbb{CP}^n spaces admit a Kähler structure such that the two-dimensional \mathbb{CP}^n models admit a supersymmetric extension with two supersymmetries. These models contain 4-fermi interactions and the Dirac operator is given by the linearized field equation for the fermions. We calculate the zero modes of this operator. There exists always one zero mode with squared amplitude being proportional to the action density of the twisted

Email addresses: wieland@theorie3.physik.uni-erlangen.de (Wieland Brendel), falk.bruckmann@physik.uni-regensburg.de (Falk Bruckmann), lukas.janssen@uni-jena.de (Lukas Janssen), wipf@tpi.uni-jena.de (Andreas Wipf), christian.wozar@uni-jena.de (Christian Wozar)

instanton.

We supplement our analytic studies by numerical simulations. With known algorithms we produce typical field configurations for various $\mathbb{C}P^n$ models with twisted boundary conditions. Then we apply standard lattice cooling techniques to extract the instantons and their constituents from a given (thermalized) configuration. Again we find that an instanton of charge k consists of $k(n+1)$ constituents. How the corresponding instanton constituents in Yang-Mills theories emerge in the process of cooling/smearing has been studied in [13, 14, 15, 16, 17, 18]. Next we compute and analyze the zero modes of the overlap Dirac operator. We find good agreement between our numerical and analytical results.

Our results demonstrate that $\mathbb{C}P^n$ models and Yang-Mills theories share one more common feature: in both models the twisted instantons generically split into well-separated and almost static constituents and in both models the fermionic zero modes trace these constituents. In $SU(N)$ Yang-Mills theories the number of constituents is given by k and the rank whereas for $\mathbb{C}P^n$ models it is given by k and by n . On the lattice the fermionic zero modes are excellent filters for the constituents. Even without much cooling the zero modes detect the constituents of the fully cooled configurations.

2. The $\mathbb{C}P^n$ model in the continuum and on the lattice

The two-dimensional $\mathbb{C}P^n$ model [19, 20] can be formulated in terms of a complex $(n+1)$ -vector $u = (u_0, \dots, u_n)^T$ subject to the constraint $u^\dagger u = 1$. The Euclidean action is given by

$$S = \frac{2}{g^2} \int d^2x (D_\mu u)^\dagger D_\mu u, \quad D_\mu = \partial_\mu - iA_\mu. \quad (1)$$

It is invariant under local $U(1)$ gauge transformations

$$u_j(x) \mapsto e^{i\lambda(x)} u_j(x), \quad A_\mu(x) \mapsto A_\mu(x) + \partial_\mu \lambda(x), \quad (2)$$

as well as global transformations

$$u_j(x) \mapsto \mathcal{U}_{jl} u_l(x) \quad (3)$$

with a constant matrix $\mathcal{U} \in U(n+1)$. The gauge field A_μ can be eliminated from the action by using its algebraic equation of motion,

$$A_\mu = -iu^\dagger \partial_\mu u. \quad (4)$$

The integer-valued instanton number,

$$Q = \int d^2x q(x) \quad \text{with} \quad q(x) = \frac{1}{2\pi} \epsilon_{\mu\nu} \partial_\mu A_\nu(x), \quad (5)$$

can be interpreted as the quantized magnetic flux in a fictitious third dimension. At infinity u must approach a pure gauge, $u(x) \rightarrow e^{i\lambda(x)} c$ and Q is just the winding number of the map $x \rightarrow e^{i\lambda(x)}$ at infinity, an element of the first homotopy group of $U(1)$.

Configurations minimizing the action in $S \geq 4\pi|Q|/g^2$ are called *instantons*. They fulfill first order *self-duality equations*.

The most general instanton solution with instanton number $Q = k \in \mathbb{N}$ can be written in homogeneous coordinates v_j as

$$u_j(x) = \frac{v_j(z)}{|v(z)|}, \quad j = 0, \dots, n, \quad (6)$$

with $\{v_j\}$ a set of polynomials of the complex coordinate $z = x_1 + ix_2$ with no common root and maximum degree k . The topological charge density of an instanton configuration then reads

$$q(x) = \frac{1}{4\pi} \Delta \ln |v(z)|^2. \quad (7)$$

Lattice formulation

For the bosonic model the lattice regularization can be obtained as described in [21, 22]. After introducing the matrix-valued gauge invariant field

$$P(x) = u(x)u^\dagger(x), \quad (8)$$

which projects onto the one-dimensional subspace spanned by u , one finds

$$\text{tr} [\partial_\mu P \partial_\mu P] = 2\partial_\mu u^\dagger \partial_\mu u + 2(u^\dagger \partial_\mu u)^2 = g^2 \mathcal{L}. \quad (9)$$

This equation, valid for the model defined on a continuous space-time, is discretized naively with the forward derivative, $\partial_\mu P \mapsto P_{x+\hat{\mu}} - P_x$, such that

$$\text{tr} [\partial_\mu P \partial_\mu P] \mapsto 2d - 2 \sum_\mu \text{tr} [P_x P_{x+\hat{\mu}}]. \quad (10)$$

Therefore, the action, up to an irrelevant additive constant, takes the form

$$S = -\frac{2}{g^2} \sum_{x,\mu} \text{tr} [P_x P_{x+\hat{\mu}}] = -\frac{2}{g^2} \sum_{x,\mu} |u_x^\dagger u_{x+\hat{\mu}}|^2. \quad (11)$$

The simulations of the lattice models have been performed with the help of an overrelaxation algorithm [22]. In addition, to investigate the topological properties, we cooled the lattice configurations [23]. For a given configuration one *cooling step* consists of minimizing the action locally on a randomly chosen site x . This is achieved by constructing $Q_x = \sum_\mu (P_{x+\hat{\mu}} + P_{x-\hat{\mu}})$ and replacing u_x by the eigenvector corresponding to the largest eigenvalue of Q_x . A *cooling sweep* corresponds to one cooling step per lattice site on average. Using this procedure the instanton constituents naturally emerge from the locally fluctuating fields.

For the topological charge on the lattice we used the geometric definition in [24] leading to an integer-valued instanton number. This definition and the chosen lattice action are sufficient for the analysis of global topological properties in the vicinity of classical configurations. Thus, we are not affected by the improper scaling behavior of the dynamical $\mathbb{C}P^n$ models with $n \leq 2$ [25].

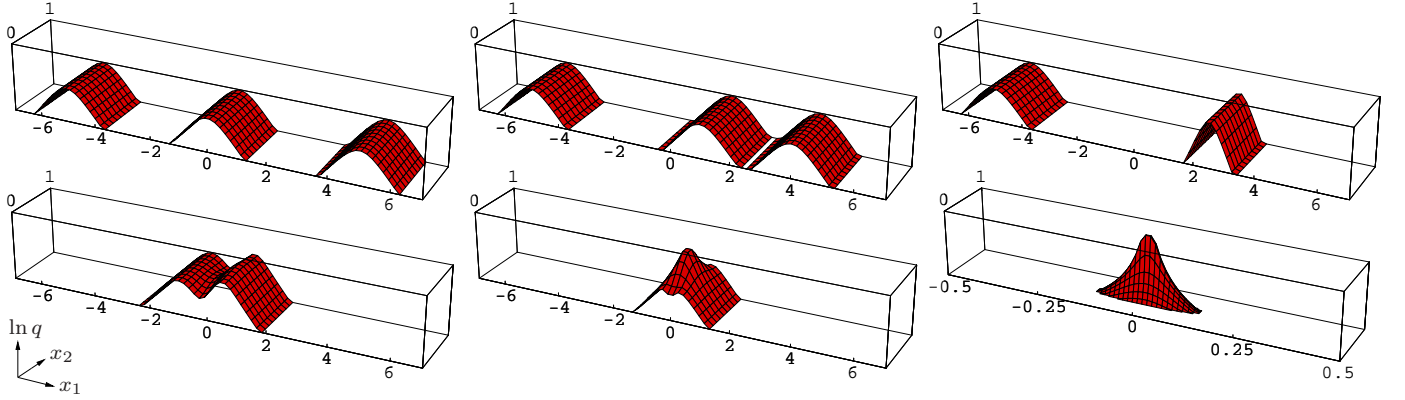


Figure 1: (Color online.) Logarithm of the topological density for the 1-instanton solution of the \mathbb{CP}^2 model (see (7) and (19)) with symmetric constituents, $\mu_1 = \mu_2 - \mu_1 = 1 - \mu_2 = 1/3$ (cut off below e^{-5}). The parameters λ_i are chosen such that the constituents are localized according to (22) from left to right at $(a_1, a_2, a_3) = (-5, 0, 5), (-5, 1, 4), (-5, 7, -2)$ (first line) and $(-1, 0.5, 0.5), (0, 0, 0), (3, -1, -2)$ (second line). Note that the x_1 -range has been changed in the lower right panel.

3. Instantons at finite temperature

For a quantum system at inverse temperature β we identify $z \sim z + i\beta$. Since β is the only length scale in the problem we measure all lengths in units of β . In particular the coordinates become dimensionless and we identify $z \sim z + i$. Periodic k -instanton solutions ('calorons') are given by [26, 27]

$$v_{\text{per}}(z) = b^{(0)} + b^{(1)} e^{2\pi z} + \dots + b^{(k)} e^{2\pi k z}. \quad (12)$$

By a global $U(n+1)$ symmetry transformation one can rotate v_{per} such that the constant (and per assumption non-vanishing) vector $b^{(k)} \in \mathbb{C}^{n+1}$ points in the 0-direction, $b_j^{(k)} = b_0^{(k)} \delta_{j0}$.

The *twisted model* is only quasi-periodic in the imaginary time direction. This means that the components v_j of v are periodic up to phases $e^{2\pi i \mu_j}$ with $\mu_j \in [0, 1)$, i.e., the vectors v and u are periodic up to a diagonal element of the global symmetry $U(n+1)$. The $U(n+1)$ -invariants like $|v|$ and A_μ and hence also q stay periodic. Without loss of generality we assume the phases to be ordered according to $\mu_0 \leq \mu_1 \leq \dots \leq \mu_n$.

For the general solutions of the twisted model we consider the Fourier ansatz

$$v_j(z) = e^{2\pi \mu_j z} \sum_{s=-\infty}^{\infty} b_j^{(s)} e^{2\pi s z} \quad (13)$$

and demand the coefficients $b_j^{(s)}$ to be non-vanishing only for a finite range of s (for each component j). This is because the corresponding maximum and minimum of the powers

$$\kappa_{\max} = \max_{j, s: b_j^{(s)} \neq 0} (s + \mu_j), \quad \kappa_{\min} = \min_{j, s: b_j^{(s)} \neq 0} (s + \mu_j) \quad (14)$$

then yield a finite topological charge Q . According to (7) one has to compute the following surface integrals

$$\begin{aligned} Q &= \frac{1}{4\pi} \int_0^\beta dx_2 \partial_1 \ln |v|^2 \Big|_{x_1 \rightarrow -\infty}^{x_1 \rightarrow \infty} \\ &= \kappa_{\max} - \kappa_{\min} \\ &\in \mathbb{N}_0 + \{\mu_j - \mu_l \mid j, l = 0, \dots, n\}. \end{aligned} \quad (15)$$

Hence the total topological charge in the twisted model can have a fractional part, whose values are restricted by the boundary conditions. By a global transformation we enforce κ_{\min} to be taken on in the 0th component and by a (non-periodic) local transformation we further set $\mu_0 = 0$ and $\kappa_{\min} = 0$, such that $Q = \kappa_{\max}$. According to Eq. (6), these powers also govern the asymptotic values of the fundamental fields u_j .

In the following we will mainly analyze *twisted instantons* with integer-valued instanton number $Q = k \in \mathbb{N}$. They are obtained by $\kappa_{\max} = k$ taken on in the 0th component, i.e., the highest coefficient $b^{(k)}$ points in the 0-direction, $b_j^{(k)} = b_0^{(k)} \delta_{j0}$. Thus one can obtain the components v_j by multiplying each component $v_{\text{per},j}$ from (12) with $\exp(2\pi \mu_j z)$, which yields

$$v(z) = \Omega v_{\text{per}}(z), \quad \Omega = \text{diag}(e^{2\pi \mu_0 z}, \dots, e^{2\pi \mu_n z}). \quad (16)$$

For $n = 1$ the known twisted unit charged instanton solution [5] can be recovered in terms of the gauge invariant field

$$\frac{v_1(z)}{v_0(z)} = \frac{b_1^{(0)} e^{2\pi \omega z}}{b_0^{(0)} + b_0^{(1)} e^{2\pi z}}. \quad (17)$$

We made use of $\mu_0 = 0$ and $b_1^{(1)} = 0$ and denoted μ_1 by ω .

3.1. One-instanton sector

In order to explore the topological density of the instantons we first consider solutions with unit charge $Q = k = 1$. We multiply v by a constant such that $b_0^{(0)} = 1$ and afterwards shift the Euclidean time x_2 such that $b_0^{(1)}$ becomes real and non-negative. For this choices the density $|v|^2$ only depends on the absolute values $\lambda_j = |b_j^{(0)}|$ with $j = 0, 1, \dots, n$. If, in addition, we define $\lambda_{n+1} = |b_0^{(1)}|$ and $\mu_{n+1} = 1$, then it can be written in the condensed form

$$|v(z)|^2 = \sum_{i=0}^{n+1} \lambda_i^2 e^{4\pi \mu_i x_1} + 2\lambda_{n+1} e^{2\pi x_1} \cos(2\pi x_2). \quad (18)$$

The corresponding topological charge density splits into $n+1$ constituents at most. For \mathbb{CP}^2 this is illustrated in Fig. 1 which shows $\ln q(x)$ for various choices of the parameters λ_i .

For the general \mathbb{CP}^n models the occurrence of the constituents can be understood geometrically. To see this more clearly we write

$$|v(z)|^2 = \sum_{i=0}^{n+1} e^{p_i(x_1)} + 2e^{\tilde{p}(x_1)} \cos(2\pi x_2), \quad (19)$$

with

$$\begin{aligned} p_i(x_1) &= 4\pi\mu_i x_1 + 2\ln\lambda_i, \\ \tilde{p}(x_1) &= 2\pi x_1 + \ln\lambda_{n+1}. \end{aligned} \quad (20)$$

In particular

$$\begin{aligned} p_0(x_1) &= 0, \\ p_{n+1}(x_1) &= 4\pi x_1 + 2\ln\lambda_{n+1} = 2\tilde{p}(x_1). \end{aligned} \quad (21)$$

We compare the graphs of these $n+3$ linear functions, see Figs. 2–4 for three examples in the \mathbb{CP}^2 model amounting to five exponential terms.

The dominant contribution to $|v|^2$ in (19) at a fixed point x_1 comes from the exponential term whose graph is above the lines defined by the other exponential terms. Hence $\ln|v|^2$ is piecewise linear in the direction x_1 up to exponentially small corrections that are maximal in transition regions, where the highest lying graphs intersect.

Note that for a strictly linear $\ln|v|^2$ the topological density $q \propto \Delta \ln|v|^2$ would vanish exactly, whereas at cusps generated by intersections of linear parts the topological density would be a Dirac delta distribution (in 3+1 dimensional Yang-Mills theory a similar singular localization can be obtained in the far-field limit [28, 11]). As this is a good approximation to the actual $\ln|v|^2$, we conclude that the topological density of the twisted instantons *splits into constituents* localized at the intersection points of the lines. Because of the ordering of the μ 's, the slopes of the linear functions p_i are ordered as well. Note that for $x_1 < -1/(2\pi\mu_1) \ln\lambda_1$ the term $\exp(p_0)$ dominates such that $\ln|v| \approx 0$ on the left of all constituents. Correspondingly, $\ln|v| \approx 4\pi x_1$ on the right of all constituents.

We obtain the maximum number of constituents, if all consecutive graphs intersect separately and above the rest of the graphs, respectively. More precisely said, the twisted instanton of \mathbb{CP}^n splits into $n+1$ constituents, if, and only if, $a_1 \ll a_2 \ll \dots \ll a_{n+1}$ ¹, whereas a_i is the intersection point of the lines p_{i-1} and p_i ,

$$a_i = -\frac{\ln(\lambda_i/\lambda_{i-1})}{2\pi(\mu_i - \mu_{i-1})}, \quad i = 1, \dots, n+1, \quad (22)$$

i.e., in particular the twist parameters μ_i are distinct, $0 = \mu_0 < \mu_1 < \dots < \mu_n < \mu_{n+1} = 1$. These positions a_i are arbitrary provided the corresponding λ -parameters are chosen according to

$$\ln\lambda_i = -2\pi \sum_{l=1}^i (\mu_l - \mu_{l-1}) a_l \quad \text{with} \quad \mu_0 = 0. \quad (23)$$

¹Thereby we do not want to take the condition $a_{i-1} \ll a_i$ too literally. It is sufficient, if a_{i-1} is not close to a_i , whereas the required distance is determined by the slopes of $p_i - p_{i-1}$ and $p_{i-1} - p_{i-2}$.

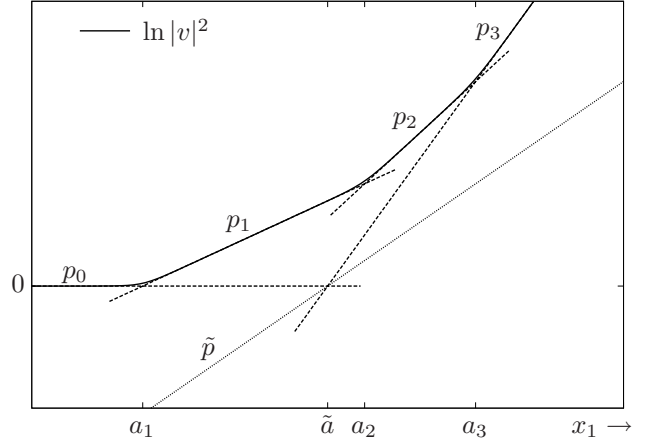


Figure 2: $\ln|v|^2$ and exponents p_i and \tilde{p} as a function of x_1 , see Eqs. (19)–(20), in the \mathbb{CP}^2 model for the case of $(a_1, a_2, a_3) = (-5, 1, 4)$, which leads to three well-separated constituents (equivalent to 2nd example in Fig. 1).

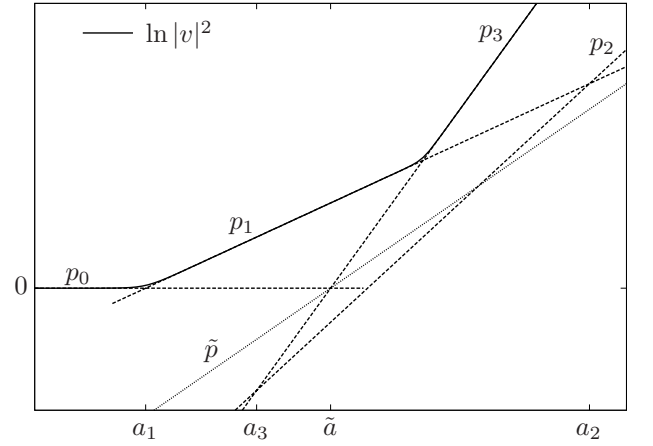


Figure 3: $\ln|v|^2$ and exponents p_i and \tilde{p} as a function of x_1 , for the case of $(a_1, a_2, a_3) = (-5, 7, -2)$, where the second and third constituent merged (equivalent to 3rd example in Fig. 1).

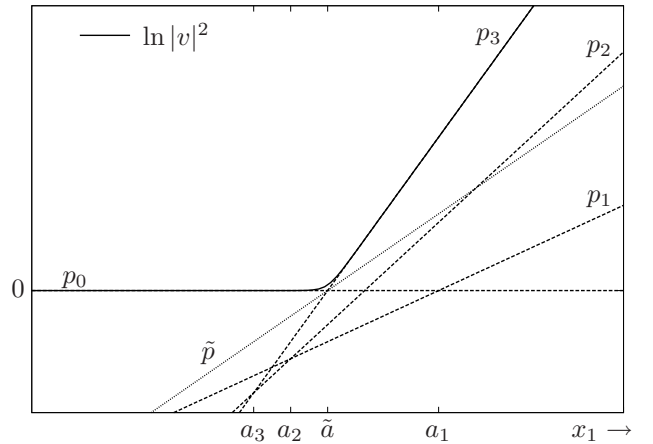


Figure 4: $\ln|v|^2$ and exponents p_i and \tilde{p} as a function of x_1 , for the case of $(a_1, a_2, a_3) = (3, -1, -2)$, where the time-dependent \tilde{p} -term becomes relevant (equivalent to 6th example in Fig. 1).

Let us discuss the case of the well-separated constituents. In the neighborhood of the intersection point a_i of the lines p_{i-1} and p_i we can approximate

$$|v(z)|^2 \approx \lambda_{i-1}^2 e^{4\pi\mu_{i-1}x_1} + \lambda_i^2 e^{4\pi\mu_i x_1}, \quad (24)$$

for x_1 not too far from the constituent i ,

$$\frac{1}{2}(a_{i-1} + a_i) \leq x_1 \leq \frac{1}{2}(a_i + a_{i+1}), \quad i = 1, \dots, n+1. \quad (25)$$

For $i = 1$ the lower bound for x_1 is $-\infty$ and for $i = n+1$ the upper bound is $+\infty$. The contribution to the topological density of the i th constituent is

$$q_{\text{const},i}(x) \approx \frac{\pi(\mu_i - \mu_{i-1})^2}{\cosh^2[2\pi(\mu_i - \mu_{i-1})(x_1 - a_i)]}. \quad (26)$$

This shape is the same for all \mathbb{CP}^n models, cf. [5] for the \mathbb{CP}^1 case. The constituent decays exponentially with characteristic length $2\pi(\mu_i - \mu_{i-1})$ (measured in units of β) away from its position a_i . It has a fractional topological charge $Q_{\text{const},i} = \mu_i - \mu_{i-1}$ and these charges add up to 1 as they should. In terms of the linear graphs the fractional topological charge is proportional to the difference of slopes of the lines that meet (which also would give the amplitude of the delta distribution mentioned above), and the total charge is the sum of all slope differences, which indeed bend the graph from p_0 with slope 0 to p_{n+1} with slope 4π eventually.

Neighboring constituents can merge adding up the fractional topological charges. This can be understood as ‘pulling down’ the line that connects the two constituents in the graph of $\ln|v|^2$, in other words by choosing the corresponding parameter λ_i small (cf. Figs. 3–4).

Under which circumstances does the time-dependence of $|v|^2$ contained in the last term of Eq. 19 (which is proportional to $\exp\tilde{p}(x_1)$) play a role? Since the three graphs of p_0 , p_{n+1} and \tilde{p} intersect at the point $(\tilde{a}, 0)$ with $2\pi\tilde{a} = -\ln\lambda_{n+1}$ we have

$$\tilde{p}(x_1) \leq \max\{p_0(x_1), p_{n+1}(x_1)\}, \quad (27)$$

such that the time-dependent \tilde{p} -term can contribute to the sum in (19) only in the neighborhood of \tilde{a} . Furthermore, all other lines have to lie below $(\tilde{a}, 0)$ (if one of the other lines p_i lies well above that point, then the topological density becomes to a good approximation static). As the slopes of the $p_i(x_1)$, $i = 1, \dots, n$ are between 0 and 1, these graphs are never dominant once they are below $(\tilde{a}, 0)$. This means that only one transition point occurs. Hence time-dependence of the instanton appears iff the topological charge is concentrated in one lump (which can be thought of as all constituents merged, cf. Fig. 4).

The case of non-distinct μ 's can be understood by considering the limit $\mu_j \rightarrow \mu_{j-1}$ for some j 's. Then the corresponding constituent becomes flatter and broader, in the limit it will be invisible and ‘massless’ (i.e., without topological charge/action; this has been ‘eaten’ by the constituent $j+1$). In this spirit we also recover the periodic solution² with $\mu_0 = \mu_1 = \dots =$

$\mu_n = 0$: The resulting topological density then consists of only one constituent with unit charge, which can, but does not have to be time-dependent (depending on where the invisible, massless constituents are localized, see also the first row in Fig. 1 of [5]). This can be demonstrated by means of Fig. 2, i.e., based on the case of well-separated constituents: The limit is taken by sending the slopes of the graphs of p_1 and p_2 to 0. If all positions a_i are kept constant (by adjusting the λ -parameters), then $p_{1,2} \rightarrow 0$ (as functions) and the resulting topological density of the periodic solution is equivalent to the case of all constituents merged in the twisted model, cf. Fig. 4 and Fig. 1 (lower right panel). If the limit is taken with all λ -parameters kept constant (i.e., by sending the positions $a_{1,2}$ to $-\infty$), then $p_{1,2} \rightarrow 2\ln\lambda_{1,2}$ can lie well above 0 in the limit and the topological density remains static, though it consists of only one unit charged constituent.

Finally, we want to mention the possibility of generating solutions with topological charge less than 1 from these instantons. Technically one has to avoid the asymptotics $\ln|v| \approx 4\pi x_1$ for large x_1 (we want to stay in the gauge where $\kappa_{\min} = 0$ and hence keep the asymptotics for small x_1). Hence, if the corresponding parameter $\lambda_{n+1} = |b_0^{(1)}|$ is vanishing (in the Fourier ansatz there is no integer phase $e^{2\pi z}$), then the total topological charge of the configuration is less than 1. A phase with $\kappa_{\max} < 1$ then gives the total topological charge (i.e., governs the asymptotics for large x_1). Also these configurations consist of constituents with the same formulae for locations, sizes and charges. The number of constituents varies from n down to 1, depending on how many of the remaining parameters λ are zero (in the graph the corresponding lines and intersection points are missing).

Interestingly, all these configurations have in common that the constituents in them are *ordered along the noncompact direction*. This has already been observed in [5] and substantiated by topological considerations. Here it can best be understood from Eq. (22). The fractional charge of the i th constituent, $\mu_i - \mu_{i-1}$, is fixed by the twist in the boundary condition. These charges can be realized in isolation only if the ordering of their positions, $a_1 \ll \dots \ll a_{n+1}$, applies. If some a_i do not obey this ordering, then constituents emerge with the sum of the individual fractions as their topological charge. In other words, ‘pulling a constituent through a neighboring one’ results not in a different ordering but in joining the constituents to a bigger one, cf. Fig. 1 (upper and lower right panels).

Notice that by giving up our choice $\kappa_{\min} = 0$ we can rearrange the constituents cyclically; this can become relevant on the lattice, where x_1 is of course periodic.

This ordering is of course related to the selfduality which dictates that all solutions are functions of $x_1 + ix_2$; antiselfdual solutions will have the opposite ordering. We therefore believe that this phenomenon is particular to 1+1 Euclidean dimensions.

²In Yang-Mills theories this amounts to the Harrington-Shepard calorons [29].

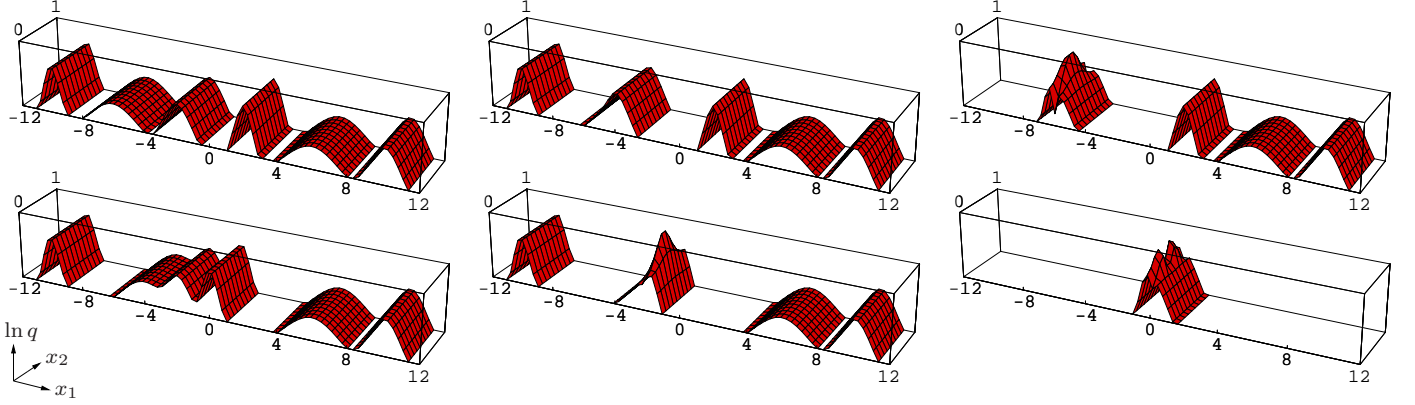


Figure 5: (Color online.) Logarithm of the topological density for the charge-2 instanton of \mathbb{CP}^2 , with non-symmetric constituents, $\mu_1 = 0.55$, $\mu_2 - \mu_1 = 0.15$, $1 - \mu_2 = 0.3$. The positions of the constituents from left to right are $(a_1, a_2, a_3, a_4, a_5, a_6) = (-10, -6, -2, 2, 6, 10)$, $(-10, -4, -4, 2, 6, 10)$, $(-6, -6, -6, 2, 6, 10)$ (first line) and $(-10, -4, -2, 0, 6, 10)$, $(-10, -2, -2, -2, 6, 10)$, $(0, 0, 0, 0, 0, 0)$ (second line).

3.2. k -instanton sector

The general twisted instanton solution (12), (16) with integer-valued topological charge k corresponds to the norm

$$|v(z)|^2 = \sum_{i=0}^{k(n+1)} e^{p_i(x_1)} + 2 \sum_{s=1}^k \sum_{i=0}^{(k-s)(n+1)} e^{\tilde{p}_i^{(s)}(x_1)} \times \cos(2\pi s x_2 + \varphi_{i+s(n+1)} - \varphi_i), \quad (28)$$

where we introduced

$$\begin{aligned} p_i(x_1) &= 4\pi\mu_i x_1 + 2 \ln \lambda_i, \\ \tilde{p}_i^{(s)}(x_1) &= 2\pi(2\mu_i + s)x_1 + \ln(\lambda_i \lambda_{i+s(n+1)}) \\ &= \frac{1}{2} [p_i(x_1) + p_{i+s(n+1)}(x_1)]. \end{aligned} \quad (29)$$

We encoded the two indices of $b_j^{(s)}$ into one, $i = s(n+1) + j$, and defined

$$\lambda_i = |b_j^{(s)}|, \quad \varphi_i = \arg(b_j^{(s)}), \quad \mu_i = \mu_j + s, \quad (30)$$

where $s = 0, \dots, k$, $j = 0, \dots, n$. To arrive at (28) we transformed the constant vector $b^{(k)}$ in the 0-direction. Similarly as for the one-instanton solution we conclude that the constituents are localized at the transition points of the piecewise linear function $|v(z)|^2$. The topological density thus splits into at most $k(n+1)$ constituents. Well-separated constituents are static and exponentially localized at a_i , $i = 1, \dots, k(n+1)$, given in an analogous manner as in the 1-instanton case, cf. Eq. (22). The constituents carry the fractional charge $\mu_i - \mu_{i-1}$ and from the periodicity of the μ 's in Eq. (30) follows that they are again ordered, see also Fig. 5, upper left panel.

Again we have

$$\tilde{p}_i^{(s)}(x_1) \leq \max \{p_i(x_1), p_{i+s(n+1)}(x_1)\}, \quad (31)$$

since the three graphs of p_i , $p_{i+s(n+1)}$ and $\tilde{p}_i^{(s)}$ all intersect at

$$\tilde{a}_i^{(s)} = -\frac{\ln(\lambda_{i+s(n+1)}/\lambda_i)}{2\pi s}. \quad (32)$$

Therefore the time-dependent term containing $\tilde{p}_i^{(s)}$ only contributes to the sum in (28) if the $s(n+1)$ constituents at the positions $a_{i+1}, \dots, a_{i+s(n+1)}$ merge to one constituent with integer charge s . The integer s thus determines the maximal frequency of the emerging constituent measured in units of the smallest possible frequency. We illustrated this behavior in Fig. 5 for 2-instanton solutions of the \mathbb{CP}^2 model. Note that the freedom φ_i of choosing the complex phase of the parameters $b_j^{(s)}$ enters only as shifts in the time dependence, Eq. (28).

3.3. Cooling of lattice data

Charge-one instantons of the \mathbb{CP}^2 model containing up to the maximal number of three constituents are reproduced with a cooling of our lattice data. The simulations were performed on a 6×100 (temporal \times spatial) lattice at coupling $g^{-2} = 2$. In the spatial direction periodic boundary conditions are imposed whereas in the temporal direction the v_j are twisted with prescribed μ_j . Then a particular configuration is cooled. During the cooling procedure configurations with $|k| = 1$ and two or more well separated constituents are fairly stable even with this type of unimproved cooling (at least up to 10^5 cooling sweeps). We also observe the typical annihilation of selfdual and anti-selfdual constituents. Only a small fraction of configurations is cooled to a state with *three* clearly separated constituents. One of these is shown in Fig. 6 at three different cooling stages. More often we end up with only *two* constituents. These results indicate that in a dynamical simulation topological objects with fractional charge (given by the twist parameters μ_j) may be as relevant as they are in Yang-Mills theories.

4. Zero modes of the Dirac operator

4.1. Minimal coupling to fermions

We extend the bosonic \mathbb{CP}^n model by introducing a massless Dirac fermion ψ , for the time being minimally coupled, such that the action has the form

$$S = \int d^2x [(D_\mu u)^\dagger D_\mu u + i\bar{\psi}\gamma^\mu D_\mu \psi]. \quad (33)$$

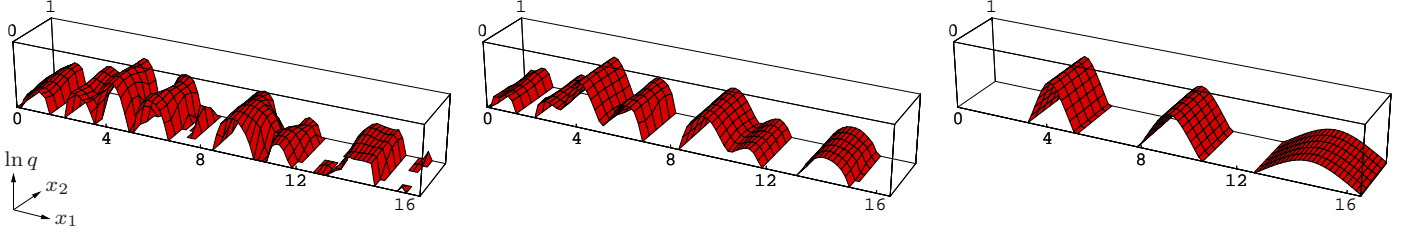


Figure 6: (Color online.) The cooling procedure is applied to a \mathbb{CP}^2 configuration of the Monte-Carlo ensemble with twists $\mu_1 = 0.15$, $\mu_2 - \mu_1 = 0.5$, $1 - \mu_2 = 0.35$. Three stable constituents emerge after several cooling sweeps (10, 25, 500 from left to right). Here only the positive part of q is shown.

We shall use the chiral representation of the γ -matrices for which $\gamma_* = -i\gamma^1\gamma^2$ is diagonal,

$$\gamma^1 = \begin{pmatrix} 0 & 1 \\ 1 & 0 \end{pmatrix}, \quad \gamma^2 = \begin{pmatrix} 0 & i \\ -i & 0 \end{pmatrix}, \quad \gamma_* = \begin{pmatrix} -1 & 0 \\ 0 & 1 \end{pmatrix}. \quad (34)$$

Splitting the Dirac spinor into chiral components $\psi = (\varphi, \chi)^T$ the Dirac equation in the background of a self-dual configuration splits into the Weyl equations

$$\begin{aligned} (\partial - u^\dagger \partial u) \varphi &= |v| \partial (|v|^{-1} \varphi) = 0, \\ (\bar{\partial} - u^\dagger \bar{\partial} u) \chi &= |v|^{-1} \bar{\partial} (|v| \chi) = 0, \end{aligned} \quad (35)$$

where ∂ and $\bar{\partial}$ denote the derivatives with respect to the complex coordinates $z = x_1 + ix_2$ and $\bar{z} = x_1 - ix_2$. It follows that the zero modes have the form

$$\varphi(x) = f(\bar{z}) |v| \quad \text{and} \quad \chi(x) = \frac{g(z)}{|v|} \quad (36)$$

with (anti-)holomorphic functions $f(\bar{z})$ and $g(z)$. Similarly as for the bosonic fields we impose quasi-periodic boundary conditions for the fermi field,

$$\psi(x_1, x_2 + 1) = e^{2\pi i \zeta} \psi(x_1, x_2) \quad \text{with} \quad \zeta \in [0, 1). \quad (37)$$

The functions f, g can be expanded in Fourier series,

$$\begin{aligned} \varphi(x) &= \sum_{s=-\infty}^{\infty} \alpha^{(s)} |v| e^{2\pi(s+\zeta)\bar{z}}, \\ \chi(x) &= \sum_{s=-\infty}^{\infty} \beta^{(s)} e^{2\pi(s+\zeta)z} / |v|. \end{aligned} \quad (38)$$

These modes are only square integrable on the cylinder if the coefficients $\alpha^{(s)}, \beta^{(s)}$ and the twist parameter ζ fulfill certain constraints. Recall that the asymptotic behavior of the general solution with charge $Q = \kappa_{\max}$ (we set $\kappa_{\min} = 0$) is

$$\lim_{x_1 \rightarrow -\infty} |v| = 1 \quad \text{and} \quad \lim_{x_1 \rightarrow \infty} |v| \propto e^{2\pi Q x_1}. \quad (39)$$

Therefore there are no normalizable left-handed zero modes φ .³ The quantum number s of the right-handed zero modes is constrained by $0 < s + \zeta < Q$.

³For anti-instantons with negative topological charge the left-handed modes become normalizable.

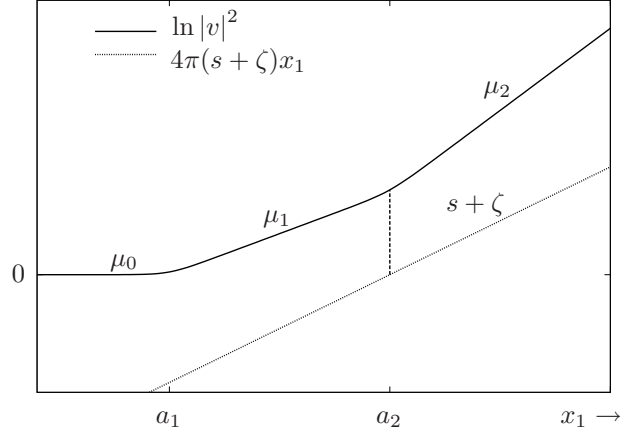


Figure 7: Piecewise linear function $\ln |v|^2$ and linear function $4\pi(s + \zeta)x_1$ for the example of $s + \zeta \in (\mu_1, \mu_2)$. For $x_1 < a_1$ the slope of $\ln |v|^2$ is $4\pi\mu_0 = 0$, for $a_1 < x_1 < a_2$ it is $4\pi\mu_1$, for $a_2 < x_1$ it is $4\pi\mu_2$. The vertical distance between the graphs is minimal at a_2 where the zero mode is localized.

This immediately leads to the *index theorem* for right-handed zero modes. For integer topological charge we have to distinguish two cases for the fermionic phases ζ :

$$\begin{aligned} \zeta = 0 &: \quad Q - 1 \text{ zero modes}, \\ \zeta \in (0, 1) &: \quad Q \text{ zero modes}. \end{aligned} \quad (40)$$

For fractional topological charge we introduce the floor function $\lfloor \cdot \rfloor : \mathbb{R} \rightarrow \mathbb{Z}$ and the fractional part $\{ \cdot \} : \mathbb{R} \rightarrow [0, 1)$ such that $Q = \lfloor Q \rfloor + \{Q\}$ and obtain

$$\begin{aligned} \zeta = 0 &: \quad \lfloor Q \rfloor \text{ zero modes}, \\ \zeta \in (0, \{Q\}) &: \quad \lfloor Q \rfloor + 1 \text{ zero modes}, \\ \zeta \in [\{Q\}, 1) &: \quad \lfloor Q \rfloor \text{ zero modes}. \end{aligned} \quad (41)$$

Let us further investigate the localization properties of the (right-handed) zero modes in the background of the instanton with integer charge $Q = k$. They have the explicit form

$$|\chi^{(s)}(x)|^2 = e^{4\pi(s+\zeta)x_1 - \ln |v|^2}, \quad s = 0, \dots, k-1, \quad (42)$$

with $|v|^2$ from (28). It is helpful to first consider well-separated constituents for which $\ln |v|^2$ becomes time-independent and piecewise linear,

$$\ln |v(z)|^2 \approx \{p_i(x_1) = 4\pi\mu_i x_1 + 2 \ln \lambda_i \mid a_i < x_1 < a_{i+1}\}, \quad (43)$$

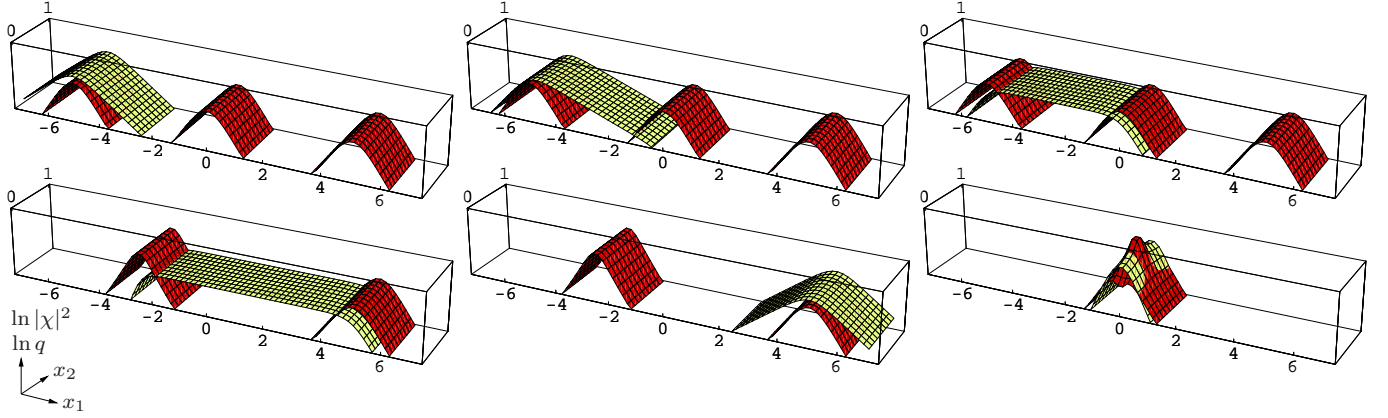


Figure 8: (Color online.) Minimally coupled fermionic zero modes (yellow/light) in the background of 1-instanton constituents (red/dark) of the CP^2 model with symmetric constituents, $\mu_1 = \mu_2 - \mu_1 = 1 - \mu_2 = 1/3$. In the first line the constituents are well-separated at $(a_1, a_2, a_3) = (-5, 0, 5)$, in the second line from left to right they are at $(-2.5, -2.5, 5)$, $(-2.5, -2.5, 5)$, $(0, 0, 0)$, i.e., two resp. three constituents have merged. The fermionic twist is $\zeta = 1/6, 1/4, 1/3$ (first line) and $2/3, 5/6, 1/2$ (second line).

as described in Sec. 3.2. Clearly, the zero mode has maximal amplitude at points where $\ln|v|^2 - 4\pi(s + \zeta)x_1$ is minimal. At these x_1 the vertical distance between the graphs of the approximately piecewise linear function $\ln|v|^2$ and the linear function $4\pi(s + \zeta)x_1$ is minimal. For $s + \zeta$ in the interval (μ_{i-1}, μ_i) the minimum is at $x_1 = a_i$ where the graphs of p_{i-1} and p_i intersect. The situation is depicted in Fig. 7.

Hence, for generic values of ζ the zero mode is *localized at one constituent*. The profile of the zero mode is symmetric about the constituent i for the particular value $s + \zeta = \frac{1}{2}(\mu_{i-1} + \mu_i)$,

$$|\chi^{(s)}(x)|^2 \propto \frac{1}{\cosh[2\pi(\mu_i - \mu_{i-1})(x_1 - a_i)]}. \quad (44)$$

Interestingly, the profile is almost constant between the i th and $(i+1)$ th constituent for $\zeta = \mu_i$. These ‘bridges’ can be understood by the fact that in this region the graphs of $\ln|v|^2$ and $4\pi(s + \zeta)x_1$ are parallel (up to exponentially small corrections) at these values of s and the fermionic phase ζ .

Altogether the zero modes walk along the ordered set of constituents when changing the fermionic phase ζ . With phases at the bounds $\zeta = 0$ resp. $\zeta = 1$ (or $\zeta = \{Q\}$ for configurations with fractional charge) the zero modes become constants asymptotically. In other words, these zero modes have ‘bridges’ coming from $-\infty$ resp. reaching out to $+\infty$ and hence are not normalizable.

Similar arguments apply if two or more constituents merge. A few examples are given in Fig. 8.

4.2. Zero modes on the lattice

Using the overlap operator with quasi-periodic boundary conditions for the $U(1)$ gauge field we are able to analyze its zero modes [30] in the background given by the cooled lattice configurations. Even for moderately cooled configurations do the zero modes reflect the position of the fully cooled instanton constituents for specific boundary conditions (see Fig. 9). Therefore the lattice results are in full agreement with the analytical

results and in addition the fermionic zero modes are excellent tracers for instanton constituents for mildly cooled configurations.

4.3. Supersymmetric coupling to fermions

The supersymmetric CP^n model [31, 32] contains $n + 1$ Dirac fermion fields ψ_j , $j = 0, \dots, n$, in addition to the complex scalar fields u_j . Its action is

$$S = \int d^2x \left\{ (D_\mu u)^\dagger (D_\mu u) + i\bar{\psi}\gamma^\mu D_\mu \psi + \frac{1}{4} \left[(\bar{\psi}\psi)^2 - (\bar{\psi}\gamma_5\psi)^2 - (\bar{\psi}\gamma^\mu\psi)(\bar{\psi}\gamma_\mu\psi) \right] \right\}, \quad (45)$$

where u and ψ are constrained by

$$u^\dagger u = 1, \quad u^\dagger \psi = \bar{\psi} u = 0. \quad (46)$$

Introducing Weyl spinors, $\psi = (\varphi, \chi)^T$, the model is invariant under the on-shell $\mathcal{N} = (2, 2)$ supersymmetry transformations

$$\begin{aligned} \delta u &= \varepsilon_1 \varphi - \varepsilon_2 \chi, \\ \delta \varphi &= +2i\bar{\varepsilon}_1 \bar{D}u - \bar{\varepsilon}_1 (\bar{\varphi}\varphi)u + \bar{\varepsilon}_2 (\bar{\chi}\chi)u, \\ \delta \chi &= -2i\bar{\varepsilon}_2 Du + \bar{\varepsilon}_2 (\bar{\chi}\chi)u - \bar{\varepsilon}_1 (\bar{\varphi}\chi)u, \end{aligned} \quad (47)$$

with the covariant derivative

$$D = \partial - u^\dagger \partial u \quad \text{and} \quad \bar{D} = \bar{\partial} - u^\dagger \bar{\partial} u \quad (48)$$

and anticommuting parameters $\varepsilon_{1,2}$ satisfying $\varepsilon_2^* = \bar{\varepsilon}_1$ and $\varepsilon_1^* = \bar{\varepsilon}_2$. Both spinors φ and χ have $n + 1$ components.

The *linearized* Dirac equation in an external u -field splits into two Weyl equations,

$$(1 - uu^\dagger) D\varphi = 0 \quad \text{and} \quad (1 - uu^\dagger) \bar{D}\chi = 0. \quad (49)$$

For an instanton background with $u = v(z)/|v|$ the Weyl equations simplify to

$$(1 - P_v) \partial \left(|v|^{-1} \varphi \right) = (1 - P_v) \bar{\partial} (|v| \chi) = 0, \quad (50)$$

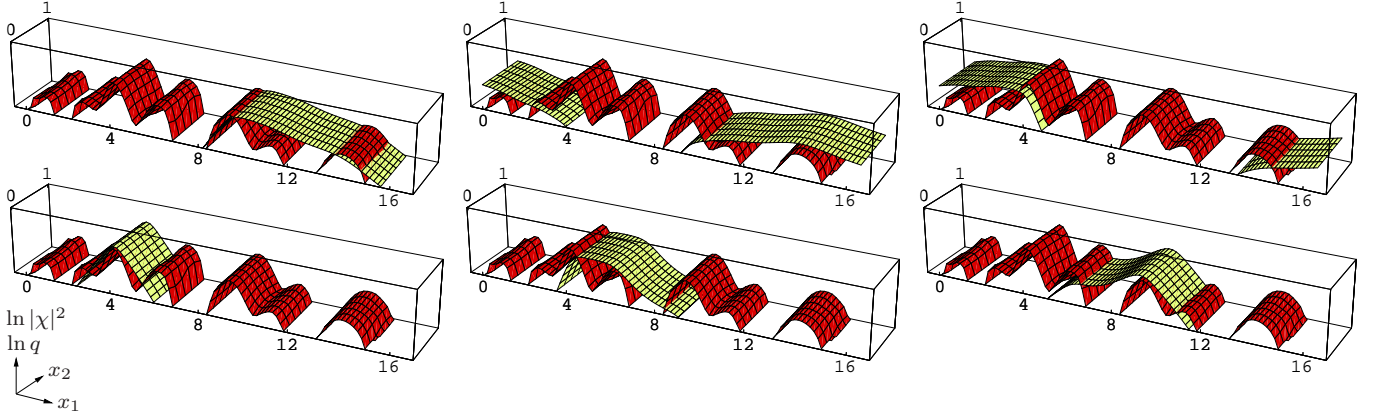


Figure 9: (Color online.) Fermionic zero modes of the overlap operator for the \mathbb{CP}^2 model with twists $\mu_1 = 0.15$, $\mu_2 - \mu_1 = 0.5$, $1 - \mu_2 = 0.35$ after application of 25 cooling sweeps (compare to Fig. 6, middle panel). The fermionic twist is $\zeta = 0, 0.075, 0.15$ (first line) and $\zeta = 0.4, 0.65, 0.825$ (second line).

where P_v projects onto the holomorphic $v(z)$,

$$P_v = uu^\dagger = \frac{vv^\dagger}{|v|^2}. \quad (51)$$

It follows that a left-handed solution reads

$$\varphi(x) = |v| f(\bar{z}), \quad (52)$$

where $f(\bar{z})$ is an arbitrary vector of anti-holomorphic functions orthogonal to v . None of these solutions is normalizable. With the help of $P_v \bar{\partial} P_v = \bar{\partial} P_v$ one shows that a right-handed solution has the form

$$\chi(x) = \frac{1}{|v|} (1 - P_v) g(z), \quad (53)$$

where $g(z)$ is a vector of holomorphic functions. In order not to break supersymmetry g must fulfill the same boundary conditions as the instanton solution v . Therefore, the choice of fermionic twists is very limited here. Each function g can be constructed by linear combination of the basis elements $\{g^{(j,s)}\}$ defined by

$$g^{(j,s)}(z) = e^{2\pi(s+\mu_j)z} e_j, \quad j = 0, \dots, n, \quad s \in \mathbb{Z}, \quad (54)$$

where e_j is the unit vector pointing in direction j . For the corresponding zero modes the squared norm is

$$|\chi^{(j,s)}|^2 = \frac{e^{4\pi(s+\mu_j)x_1}}{|v|^4} \sum_{l \neq j}^n |v_l|^2. \quad (55)$$

Normalizability of the zero mode in the k -instanton background requires

$$s = \begin{cases} 0, 1, \dots, k & \text{for } j = 0, \\ 0, 1, \dots, k-1 & \text{for } j = 1, \dots, n. \end{cases} \quad (56)$$

In the case of well-separated instanton constituents we can write

$$|\chi^{(i)}|^2 \approx \frac{1}{|v|^4} \sum_{l \bmod (n+1) \neq i}^{k(n+1)} e^{p_l(x_1) + 4\pi\mu_i x_1}, \quad (57)$$

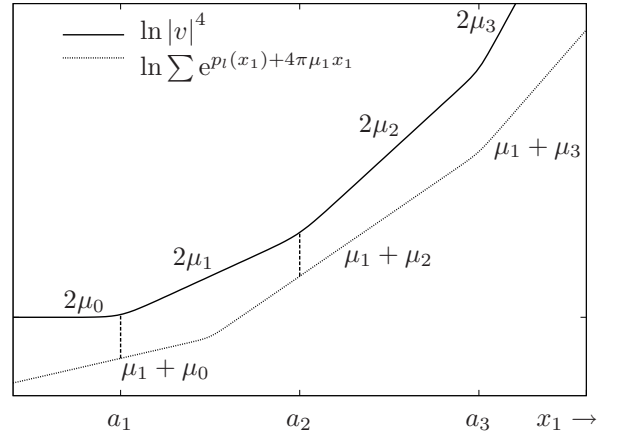


Figure 10: Logarithm of denominator and numerator of $|\chi^{(1)}|^2$ in (57). The zero mode has two maxima of equal amplitude at a_1 and a_2 .

where we introduced $\chi^{(i)} = \chi^{(j,s)}$ for $i = s(n+1) + j$. The linear functions $p_l(x_1)$ are given in (29). Again the maximum of $|\chi^{(i)}|$ is easily found by considering the graphs of the linear functions $2p_l(x_1)$ and $p_l(x_1) + 4\pi\mu_i x_1$. In a logarithmic plot both the numerator and denominator of $|\chi^{(i)}|$ are piecewise linear. For $x_1 < a_i$ the slope of the numerator is larger and for $x_1 > a_{i+1}$ the slope of the denominator is larger. This is illustrated in Fig. 10. Simple geometric arguments about these graphs reveal, that the zero modes $\chi^{(i)}$ with $0 < i < k(n+1)$ split into two constituents located at a_i and a_{i+1} , which have the same amplitude, but decay with different lengths. The zero modes $\chi^{(0)}$ and $\chi^{(k(n+1))}$ have only one maximum at a_1 and $a_{k(n+1)}$, respectively. Some examples are plotted in Fig. 11. The general right-handed zero mode has the form

$$\chi = \sum_{i=0}^{k(n+1)} \beta_i \chi^{(i)}. \quad (58)$$

Its (squared) norm splits into $k(n+1)$ or less constituents. They have the same analytic form $\propto \cosh^{-2} [2\pi Q_{\text{const},i}(x_1 - a_i)]$ and are located at the same positions a_i as the instanton constituents.

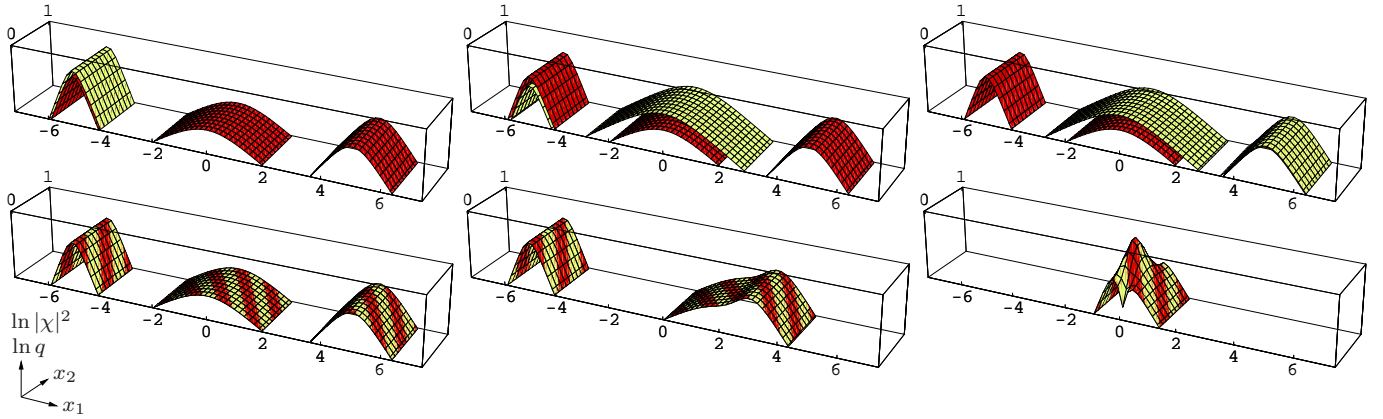


Figure 11: (Color online.) Supersymmetric coupled fermionic zero modes (yellow/light) in the background of 1-instanton constituents (red/dark) in the \mathbb{CP}^2 model with twist parameters $\mu_1 = 0.55$, $\mu_2 - \mu_1 = 0.15$, $1 - \mu_2 = 0.3$. In the first line the zero modes $\chi^{(0)}$, $\chi^{(1)}$ and $\chi^{(2)}$ (from left to right) with instanton locations $(a_1, a_2, a_3) = (-5, 0, 5)$. In the second line the half-BPS state χ_{inst} with instanton locations $(-5, 0, 5)$, $(-5, 2, 3)$, $(0, 0, 0)$ (from left to right).

There exists always a particular zero mode, whose (squared) norm is proportional to the topological density

$$q = \frac{1}{4\pi} \Delta \ln |v|^2 = \frac{1}{\pi} \frac{|v|^2 |\partial v|^2 - |v^\dagger \partial v|^2}{|v|^4}. \quad (59)$$

Namely, since the squared norm of χ in (53) is

$$|\chi|^2 = \frac{|v|^2 |g|^2 - |v^\dagger g|^2}{|v|^4}, \quad (60)$$

we obtain the exact relation

$$|\chi(x)|^2 = \pi q(x) \quad (61)$$

for the zero mode with $g = \partial v$, which means that $\beta_i \propto \mu_i \lambda_i$ in Eq. (58).

The occurrence of this particular zero mode can also be understood as follows: Any instanton background breaks half of the supersymmetry, namely the one generated by the parameter $\bar{\varepsilon}_2$. If we transform the configuration $u_{\text{inst}} = v(z)/|v|$, $\psi_{\text{inst}} = 0$ with the broken symmetry then $\delta\psi_{\text{inst}}$ is inevitably a zero mode of the Dirac operator for the action is invariant under the supersymmetry transformation. This way we obtain a non-vanishing right-handed zero mode

$$\delta\chi_{\text{inst}} = -2i\bar{\varepsilon}_2 Du \propto \frac{1}{|v|} (1 - P_v) \partial v, \quad (62)$$

that is a zero mode with $g \propto \partial v$. Except for irrelevant prefactors, this is exactly the zero mode whose squared norm is equal to the topological density of the instanton.

5. Conclusions

In the present work we constructed and analyzed the integer-charged instantons for twisted \mathbb{CP}^n models on a cylinder. The twisted instantons with charge k support $k(n+1)$ constituents. If these constituents are well-separated then they become static lumps. The fractional charges and the shapes of the constituents

topological profile are governed by the phases in the boundary condition (and the scale β). The constituent positions are related to the collective parameters of the twisted instanton and hence free up to the demand that for all constituents to be present their positions must be ordered.

Neighboring constituents can merge adding up their charges. If at least $n+1$ constituents merge then the resulting lump becomes time-dependent. For a composite object containing multiples of $n+1$ constituents time-dependent terms with higher frequencies contribute, respectively.

Our analytic findings are in complete agreement with the corresponding numerical ones. The latter were obtained by cooling lattice configurations of the twisted model with a non-vanishing topological charge.

We determined all fermionic zero modes in the background of the twisted instantons. This has been achieved for minimally coupled fermions satisfying quasi-periodic boundary conditions in the Euclidean time direction. We found that, similarly as for gauge theories, the zero modes are localized at the positions of the constituents and that they may jump from one constituent to the neighboring one if the boundary conditions for the fermions are changed. Again we compared our analytical findings to numerical results. To that aim we determined the zero modes of the overlap Dirac operator for lattice configurations with different degrees of cooling. Again we find full agreement between our analytical and numerical results, in close analogy with the corresponding situation for $SU(N)$ Yang-Mills theories.

In the supersymmetric \mathbb{CP}^n model the Dirac fermions transform according to the fundamental representation of the global $U(n+1)$ symmetry group. The linearized field equations for the $n+1$ fermion-flavors define a supersymmetric Dirac operator. We studied the square integrable zero modes of this operator and showed that they generically split into $k(n+1)$ constituents with maxima at the locations of the instanton constituents. There exists always a particular zero mode whose norm squared is equal to the topological charge density of the supporting instanton. This zero mode is generated by the half-broken supersymmetry. We did not elaborate on the contribution of the constituents and zero modes to the central charge of

the $(2, 2)$ SUSY algebra.

Our results are in close parallel to the corresponding findings in $SU(N)$ gauge theories. But since twisted instantons, their constituents and the fermionic zero modes in $\mathbb{C}P^n$ models are much simpler as in gauge theories our results may be useful to shed further light on the relevant degrees of freedom in strongly coupled models at finite temperature. The next natural step would be to include quantum fluctuations about twisted instantons to study the quantum corrections to the constituent picture.

In the $SU(N)$ gauge theory there is a beautiful construction of the constituents based on the Nahm transform [6]. We believe that a similar construction, with Nahm transform as introduced in [4], could further simplify the construction of instanton constituents for twisted $\mathbb{C}P^n$ models.

Similar aspects of twisted $\mathbb{C}P^n$ models (such as loop groups) are discussed in a simultaneous paper [33].

Acknowledgments

We thank Michael Thies for discussions and Ulrich Theis for pointing us to the BPS-interpretation of one of the zero modes of the supersymmetric Dirac operator. W. Brendel, L. Janssen and C. Wozar thank for the support by the Studienstiftung des deutschen Volkes. This work has been supported by the DFG grants Wi 777/10-1 and BR 2872/4-1.

References

- [1] A. M. Polyakov, *Interaction of Goldstone Particles in Two-Dimensions. Applications to Ferromagnets and Massive Yang-Mills Fields*, Phys. Lett. **B59** (1975) 79.
- [2] A. M. Tsvetlik, *Quantum Field Theory in Condensed Matter*, Cambridge University Press, 1995.
- [3] E. Mottola and A. Wipf, *Unsuppressed Fermion Number Violation at High Temperature: an $O(3)$ Model*, Phys. Rev. **D39** (1989) 588.
- [4] M. Aguado, M. Asorey and A. Wipf, *Nahm transform and moduli spaces of CP^N -models on the torus*, Annals Phys. **298** (2002) 2 [arXiv:hep-th/0107258].
- [5] F. Bruckmann, *Instanton constituents in the $O(3)$ model at finite temperature*, Phys. Rev. Lett. **100** (2008) 051602 [arXiv:0707.0775].
- [6] T. C. Kraan and P. van Baal, *Periodic instantons with non-trivial holonomy*, Nucl. Phys. **B533** (1998) 627 [arXiv:hep-th/9805168].
- [7] K. Lee and C. Lu, *$SU(2)$ calorons and magnetic monopoles*, Phys. Rev. **D58** (1998) 025011 [arXiv:hep-th/9802108].
- [8] F. Bruckmann, D. Negradi and P. van Baal, *Instantons and constituent monopoles*, Acta Phys. Polon. **B34** (2003) 5717 [arXiv:hep-th/0309008].
- [9] F. Bruckmann, *Topological objects in QCD*, Eur. Phys. J. ST **152** (2007) 61 [arXiv:0706.2269].
- [10] M. Garcia Perez, A. Gonzalez-Arroyo, C. Pena and P. van Baal, *Weyl-Dirac Zero-Mode for Calorons*, Phys. Rev. **D60** (1999) 031901 [arXiv:hep-th/9905016].
- [11] F. Bruckmann, D. Negradi and P. van Baal, *Constituent monopoles through the eyes of fermion zero-modes*, Nucl. Phys. **B666** (2003) 197 [arXiv:hep-th/0305063].
- [12] C. Ford and J. M. Pawłowski, *Doubly periodic instanton zero modes*, Phys. Lett. **B626** (2005) 139 [arXiv:hep-th/0505214].
- [13] M. Garcia Perez, A. Gonzalez-Arroyo, A. Montero and P. van Baal, *Calorons on the Lattice: A New Perspective*, JHEP **06** (1999) 001 [arXiv:hep-lat/9903022].
- [14] E.-M. Ilgenfritz, B. V. Martemyanov, M. Müller-Preussker, S. Shcheredin and A. I. Veselov, *On the topological content of $SU(2)$ gauge fields below T_c* , Phys. Rev. **D66** (2002) 074503 [arXiv:hep-lat/0206004].
- [15] F. Bruckmann, E.-M. Ilgenfritz, B. V. Martemyanov and P. van Baal, *Probing for instanton constituents with ϵ -cooling*, Phys. Rev. **D70** (2004) 105013 [arXiv:hep-lat/0408004].
- [16] E.-M. Ilgenfritz, B. V. Martemyanov, M. Müller-Preussker and A. I. Veselov, *The monopole content of topological clusters: Have KvB calorons been found?*, Phys. Rev. **D71** (2005) 034505 [arXiv:hep-lat/0412028].
- [17] E.-M. Ilgenfritz, M. Müller-Preussker and D. Peschka, *Calorons in $SU(3)$ lattice gauge theory*, Phys. Rev. **D71** (2005) 116003 [arXiv:hep-lat/0503020].
- [18] V. G. Borynyakov, E.-M. Ilgenfritz, B. V. Martemyanov and M. Müller-Preussker, *The dyonic picture of topological objects in the deconfined phase*, arXiv:0809.2142.
- [19] H. Eichenherr, *$SU(N)$ Invariant Nonlinear Sigma Models*, Nucl. Phys. **B146** (1978) 215.
- [20] A. D’Adda, M. Lüscher and P. Di Vecchia, *A $1/n$ Expandable Series of Nonlinear Sigma Models with Instantons*, Nucl. Phys. **B146** (1978) 63.
- [21] P. Di Vecchia, A. Holtkamp, R. Musto, F. Nicodemi and R. Pettorino, *Lattice CP^{N-1} models and their large N behavior*, Nucl. Phys. **B190** (1981) 719.
- [22] U. Wolff, *Scaling topological charge in the CP^3 spin model*, Phys. Lett. **B284** (1992) 94 [arXiv:hep-lat/9205001].
- [23] B. Berg, *Dislocations and topological background in the lattice $O(3)$ sigma model*, Phys. Lett. **B104** (1981) 475.
- [24] B. Berg and M. Lüscher, *Definition and Statistical Distributions of a Topological Number in the Lattice $O(3)$ Sigma Model*, Nucl. Phys. **B190** (1981) 412.
- [25] M. Lüscher, *Does the Topological Susceptibility in Lattice Sigma Models Scale According to the Perturbative Renormalization Group?*, Nucl. Phys. **B200** (1982) 61.
- [26] I. Affleck, *The Role of Instantons in Scale Invariant Gauge Theories (II). The Short-Distance Limit*, Nucl. Phys. **B171** (1980) 420.
- [27] A. Actor, *Temperature Dependence of the CP^{N-1} Model and the Analogy with Quantum Chromodynamics*, Fortsch. Phys. **33** (1985) 333.
- [28] F. Bruckmann and P. van Baal, *Multi-caloron solutions*, Nucl. Phys. **B645** (2002) 105 [arXiv:hep-th/0209010].
- [29] B. J. Harrington and H. K. Shepard, *Periodic euclidean solutions and the finite temperature Yang-Mills gas*, Phys. Rev. **D17** (1978) 2122.
- [30] F. Niedermayer, *Exact chiral symmetry, topological charge and related topics*, Nucl. Phys. Proc. Suppl. **73** (1999) 105 [arXiv:hep-lat/9810026].
- [31] A. D’Adda, M. Lüscher and P. Di Vecchia, *Confinement and Chiral Symmetry Breaking in CP^{N-1} Models with Quarks*, Nucl. Phys. **B152** (1979) 125.
- [32] E. Witten, *Instantons, the Quark Model, and the $1/n$ Expansion*, Nucl. Phys. **B149** (1979) 285.
- [33] D. Harland, *Kinks, chains, and loop groups in the CP^n sigma models*, arXiv:0902.2303.